

# Fluid flow profile in the “orthotropic plate+compressible viscous fluid+rigid wall” system under the action of the moving load on the plate

Surkay D. Akbarov<sup>\*1,2</sup> and Tarana V. Huseynova<sup>3a</sup>

<sup>1</sup>Department of Mechanical Engineering, Yildiz Technical University, 34349, Besiktas, Istanbul, Turkey

<sup>2</sup>Institute of Mathematics and Mechanics of the National Academy of Sciences of Azerbaijan,  
AZ1141, Baku, Azerbaijan

<sup>3</sup>Ganja State University, Ganja, Azerbaijan

(Received October 9, 2019, Revised February 24, 2020, Accepted February 27, 2020)

**Abstract.** The paper studies the fluid flow profile contained between the orthotropic plate and rigid wall under the action of the moving load on the plate and main attention is focused on the fluid velocity profile in the load moving direction. It is assumed that the plate material is orthotropic one and the fluid is viscous and barotropic compressible. The plane-strain state in the plate and the plane flow of the fluid is considered. The motion of the plate is described by utilizing the exact equations of elastodynamics for anisotropic bodies, however, the flow of the fluid by utilizing the linearized Navier-Stokes equations. For the solution of the corresponding boundary value problem, the moving coordinate system associated with the moving load is introduced, after which the exponential Fourier transformation is employed with respect to the coordinate which indicates the distance of the material points from the moving load. The exact analytical expressions for the Fourier transforms of the sought values are obtained, the originals of which are determined numerically. Presented numerical results and their analyses are focused on the question of how the moving load acting on the face plane of the plate which is not in the contact with the fluid can cause the fluid flow and what type profile has this flow along the thickness direction of the strip filled by the fluid and, finally, how this profile changes ahead and behind with the distance of the moving load.

**Keywords:** fluid flow profile; orthotropic plate; compressible viscous fluid; moving load; hydro-elastic system; Fourier transform

## 1. Introduction

The fluid flow and its profile in the “plate + fluid systems” is one of the main factors for the detailed analysis of the dynamics of these systems. A characteristic feature of this flow is that it is caused by a moving load acting on the fluid through an elastic plate which is in contact with this fluid. Consequently, the mentioned flow of the fluid can also be considered as the fluid response to the moving load. Another aspect of the mentioned dynamic process is the determination of the possibilities through which it can cause the fluid flow by the action of the moving load acting on the

---

\*Corresponding author, Professor, E-mail: [akbarov@yildiz.edu.tr](mailto:akbarov@yildiz.edu.tr)

<sup>a</sup>Ph.D., E-mail: [terane.huseynova.77@mail.ru](mailto:terane.huseynova.77@mail.ru)

plate in contact with this fluid. Therefore, the subject of the present paper which relates to the determination of the influence of the problem parameters on this flow in the “orthotropic plate+compressible viscous fluid+rigid wall” hydro-elastic system has not only theoretical but also the practical significance.

Note that in earlier, the dynamics of the moving load acting on the plate+fluid systems which are taken as the model for the floating bridge was studied in the papers (Wu and Shih 1998, Fu *et al.* 2005, Wang *et al.* 2009, and others listed therein). However in these papers the fluid response to the plate on which the moving load acts, is taken into consideration within the scope the linear spring-type model, according to which, the hydrostatic force (denoted by  $R$ ) appearing as a result of the plate - fluid interaction, is determined through the relation, where is the vertical displacement of the plate and is the spring constant. It is evident that in the aforementioned investigations the fluid reaction to the moving load is taken into consideration only through this spring constant. Moreover, it is evident that the approach used in the foregoing works is a very approximate one and cannot describe fluid flow profile which appears as a result of the acting moving load on the plate. Note that such describing can be made within the scope of the approach developed in the works (Akbarov and Ismailov 2014, 2015, 2016, 2017, 2018, Akbarov *et al.* 2017, Akbarov and Panakhli 2017, Akbarov and Huseynov 2019 and others listed therein) which are employed for investigations of the dynamic response of the hydro-elastic (-viscoelastic) systems consisting of the plate, compressible viscous fluid and rigid wall to the time-harmonic moving load acting on the plate. The detailed review of these investigations is given in the paper (Akbarov 2018) and some parts of those are detailed in the monograph (Akbarov 2015). It should be indicated that in these works the motion of the fluid is described within the scope of the linearized Navier-Stokes equations and the motion of the plate within the scope of the exact equations and relations of elastodynamics. However, in these works, the concrete investigations are made for the fluid flow velocity and fluid pressure acting on the interface between the fluid and plate. Consequently, in these works, there are not any investigations on the fluid flow profile across the thickness of the strip filled with the fluid under the action of the moving load on the plate.

Note that the study of the fluid flow profile in the fluid-plate systems, in general, was not the main subject of the related investigations which were started in the paper (Lamb 1921), which studied the natural vibrations of a circular elastic “baffled” plate-still water system by utilizing the so-called “non-dimensional added virtual mass incremental” (NAVMI) method. In the papers (McLachlan 1932, Kwak and Kim 1991, Amabili and Kwak 1996, Amabili 1996, Kwak 1997, Kwak and Han 2000 and many others listed therein) it was developed the aforementioned Lamb’s investigation. It should be noted that in all these investigations the fluid is modelled as an inviscid incompressible one and the motion of the plate is described within the scope of the Kirchhoff hypothesis and the main aim of these works is to establish the magnitude of the influence of the contact of the plate with the fluid on the values of the natural vibrations of the plate.

In some subsequent investigations, it is refused from the foregoing assumptions related to the fluid properties. For instance, in the paper (Jeong and Kim 2005) it is investigated natural frequencies of a circular plate submerged in a bounded compressible fluid. Moreover, in the papers (Atkinson and Manrique de Lara 2007, Kozlovsky 2009) it is taken the viscosity of the incompressible fluid into consideration, under investigation vibration of the plate which is in contact with this fluid. The fluid viscosity is also taken into consideration in the paper (Sorokin and Chubinskij 2008) in which it is considered the infinite plate fluid system and the motion of this plate is described within the scope of the various approximate plate theories.

The model “an infinite plate - viscous fluid” is also used in the papers (Bagno *et al.* 1994, Bagno

2015 and others listed therein) and also in the papers the list and the review of which is detailed in the works (Bagno *et al.* 1997, Guz *et al.* 2016) and detailed in the monograph (Guz 2009). At the same time, in these works, the fluid is taken as compressible one and its flow is described through the linearized Navier-Stokes equations and the motion of the plate is described by utilizing the three-dimensional linearized equations of wave propagation in elastic bodies with initial stresses and within these frameworks it is studied the wave propagation in the plate-fluid system. Note that the same equations and relations were also used in the works (Akbarov and Ismailov 2014, 2015, 2016, 2017, 2018, Akbarov *et al.* 2017, Akbarov and Panakhli 2017, Akbarov and Huseynov 2019 and others listed therein), which are already noted above. We recall that in these works it was obtained the results related the stresses and velocity distribution on the interface plane between the fluid and plate in the cases where on the plate acts one of the following type load: the time-harmonic load, the moving load and the time-harmonic moving load. Note that these results can also be used as qualitative information on the pressure distribution under dynamic loading of the fluid-structure interaction systems the consideration of which was also made in the papers (Hadzalic *et al.* 2018, Kelvani *et al.* 2013, Mandal and Maity 2015 and in many others which are listed therein).

In all the reviewed above papers, except the paper (Akbarov and Huseynova 2019), it was assumed that the plate material is a homogeneous and isotropic one. In connection with this, the results obtained in these papers cannot be applied for the cases where the plate, made of composite (or anisotropic) material, is in contact with the fluid. The examples for such cases are given in the papers (Shiffer and Tagarielli 2015, Das and Kapuria 2016, Kaneke *et al.* 2018, Gagani and Echtermeyer 2019). According to this statement, it was appeared the need to develop of the foregoing investigations carried out in the papers (Akbarov and Ismailov 2014, 2015, 2016, 2017, 2018, Akbarov *et al.* 2017, Akbarov and Panakhli 2017 and others listed therein) for the cases where the plate material is anisotropic one. Such development was made in the paper (Akbarov and Huseynova 2019) in which it was investigated the forced vibration of the “orthotropic plate+compressible viscous fluid+rigid wall” system and it was established the influence of the plate material anisotropy on the interface stresses and the interface velocities.

In the present work, we attempt to develop the investigations started in the paper (Akbarov and Huseynova 2019) for the case where on the plate the moving load acts and to study the fluid flow profile across the thickness of the strip filled with this fluid. As well as to study the change of this profile with the distance from the point at which the moving load acts.

## 2. Formulation of the problem and governing field equations and relations

As in the paper (Akbarov and Huseynova 2019), consider the hydro-elastic system “orthotropic plate-layer+compressible barotropic viscous fluid+rigid wall” schematically shown in Fig. 1, according to which, the Cartesian coordinate system  $Ox_1x_2x_3$  is associated with the upper face plane of the plate. Within this coordinate system the region  $\{-\infty < x_1 < +\infty; -h < x_2 < 0; -\infty < x_3 < +\infty\}$  is occupied by the plate and the region  $\{-\infty < x_1 < +\infty; -h-h_d < x_2 < -h; -\infty < x_3 < +\infty\}$  is occupied by the fluid, where  $h$  is the plate thickness and  $h_d$  is the fluid depth, and the plane  $x_2 = -h - h_d$  illustrates the rigid wall. In Fig. 1 the  $Ox_3$  axis doesn't shown this is because it is assumed that this axis direction is perpendicular to the Fig. 1 plane and the distribution of the external forces with intensity  $P_0$  which are located on the line  $\{-\infty < x_3 < +\infty; x_1 = Vt; x_2 = 0\}$

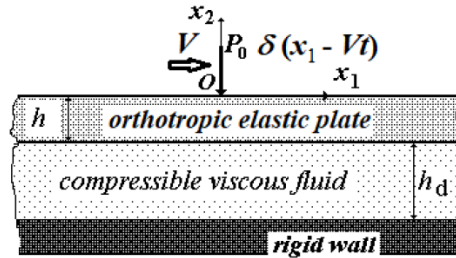


Fig. 1 The sketch of the hydro-elastic system consisting of orthotropic elastic plate, compressible viscous fluid and rigid wall under action moving load

and move along the  $Ox_1$  axis with the constant velocity  $V$  doesn't depend on the coordinate  $x_3$ . Consequently, according to this statement, it is appear the plane-strain state in the plate and plane flow of the fluid in the  $Ox_1x_2$  plane.

Assume that the plate material is an orthotropic one the elastic symmetry axes of which coincide with the coordinate axes  $Ox_1$ ,  $Ox_2$  and  $Ox_3$ , and this assuming is the main one, according to which, the formulation of the problem in the present paper differs from the that given in the paper (Akbarov and Ismailov 2015).

Thus, within the framework of the foregoing assumptions, we write the field equations and relations for the constituents of the hydro-elastic system.

The equations of motion for the plate

$$\frac{\partial \sigma_{11}}{\partial x_1} + \frac{\partial \sigma_{12}}{\partial x_2} = \rho \frac{\partial^2 u_1}{\partial t^2}, \quad \frac{\partial \sigma_{12}}{\partial x_1} + \frac{\partial \sigma_{22}}{\partial x_2} = \rho \frac{\partial^2 u_2}{\partial t^2}. \quad (1)$$

The elasticity relation

$$\sigma_{11} = a_{11}\varepsilon_{11} + a_{12}\varepsilon_{22}, \quad \sigma_{22} = a_{12}\varepsilon_{11} + a_{22}\varepsilon_{22}, \quad \sigma_{12} = 2G_{12}\varepsilon_{12}, \quad (2)$$

where

$$\begin{aligned} a_{11} &= \frac{A_{22}}{A_{11}A_{22} - A_{12}^2}, \quad a_{12} = \frac{A_{12}}{A_{11}A_{22} - A_{12}^2}, \quad a_{22} = \frac{A_{11}}{A_{11}A_{22} - A_{12}^2}, \\ A_{11} &= \frac{1 - \nu_{13}\nu_{31}}{E_1}, \quad A_{12} = -\frac{\nu_{12} + \nu_{13}\nu_{32}}{E_1}, \quad A_{22} = \frac{1 - \nu_{23}\nu_{32}}{E_1}, \\ \nu_{13}E_1 &= \nu_{31}E_3, \quad \nu_{21}E_2 = \nu_{12}E_1, \quad \nu_{32}E_3 = \nu_{23}E_2. \end{aligned} \quad (3)$$

The strain-displacement relations

$$\varepsilon_{11} = \frac{\partial u_1}{\partial x_1}, \quad \varepsilon_{22} = \frac{\partial u_2}{\partial x_2}, \quad \varepsilon_{12} = \frac{1}{2} \left( \frac{\partial u_1}{\partial x_2} + \frac{\partial u_2}{\partial x_1} \right). \quad (4)$$

The following notation is used in (3) and (4):  $E_1$ ,  $E_2$  and  $E_3$  are the modulus of elasticity of the plate material in the directions of the  $Ox_1$ ,  $Ox_2$  and  $Ox_3$  axes, respectively,  $G_{12}$  is the shear modulus in the  $Ox_1x_2$  plane,  $\nu_{ij}$  ( $i, j = 1, 2, 3$ ) is the Poisson's coefficient characterizing the shorting (the lengthening) of the material fibers in the  $Ox_i$  axis direction under stretching (under compressing) in

the  $Ox_j$  axis direction;  $\sigma_{ij}$  and  $\varepsilon_{ij}$  ( $ij = 11; 22; 12$ ) are the components of the stress and strain tensor, respectively;  $u_1$  and  $u_2$  are the components of the displacement vector in the  $Ox_1$  and  $Ox_2$  axes directions, respectively.

Thus, the closed complete system of equations and relations given in (1)-(4) are the field equations related to the motion of the orthotropic plate.

Also, consider the field equations and relations related to the fluid flow. According to the monograph (Guz 2009), it is assumed that the motion of the fluid is described with the following linearized Navier-Stokes equations.

$$\begin{aligned} \rho_0^{(1)} \frac{\partial V_i}{\partial t} - \mu^{(1)} \frac{\partial^2 V_i}{\partial x_j \partial x_j} + \frac{\partial p^{(1)}}{\partial x_i} - (\lambda^{(1)} + \mu^{(1)}) \frac{\partial^2 V_j}{\partial x_j \partial x_i} = 0, \quad \frac{\partial \rho^{(1)}}{\partial t} + \rho_0^{(1)} \frac{\partial V_j}{\partial x_j} = 0, \\ T_{ij} = (-p^{(1)} + \lambda^{(1)} \theta) \delta_{ij} + 2\mu^{(1)} e_{ij}, \quad \theta = \frac{\partial V_1}{\partial x_1} + \frac{\partial V_2}{\partial x_2}, \\ e_{ij} = \frac{1}{2} \left( \frac{\partial V_i}{\partial x_j} + \frac{\partial V_j}{\partial x_i} \right). \quad a_0^2 = \frac{\partial p^{(1)}}{\partial \rho^{(1)}}, \quad i, j = 1, 2 \end{aligned} \tag{5}$$

In (5) it is made summation with respect to the repeating indices and the following notation is used:  $\rho_0^{(1)}$  is the fluid density before perturbation,  $\rho^{(1)}$  is the perturbation of the fluid density,  $p^{(1)}$  is the perturbation of the hydrostatic pressure,  $V_1$  and  $V_2$  are the components of the fluid flow velocity vector in the directions of the  $Ox_1$  and  $Ox_2$  axes, respectively,  $T_{ij}$  and  $e_{ij}$  are the components of the stress and strain velocity tensors in the fluid,  $a_0$  is the sound velocity in the fluid,  $\lambda^{(1)}$  and  $\mu^{(1)}$  are the coefficients of the fluid viscosity.

For the solution to the equations in (5), according to the monograph (Guz 2009), it can be used the following presentation for the velocities  $V_1$ ,  $V_2$  and the pressure  $p^{(1)}$

$$V_1 = \frac{\partial \varphi}{\partial x_1} + \frac{\partial \psi}{\partial x_2}, \quad V_2 = \frac{\partial \varphi}{\partial x_2} - \frac{\partial \psi}{\partial x_1}, \quad p^{(1)} = \rho_0^{(1)} \left( \frac{\lambda^{(1)} + 2\mu^{(1)}}{\rho_0^{(1)}} \Delta - \frac{\partial}{\partial t} \right) \varphi, \tag{6}$$

where the potentials  $\varphi$  and  $\psi$  satisfy the following equations.

$$\left[ \left( 1 + \frac{\lambda^{(1)} + 2\mu^{(1)}}{a_0^2 \rho_0^{(1)}} \frac{\partial}{\partial t} \right) \Delta - \frac{1}{a_0^2} \frac{\partial^2}{\partial t^2} \right] \varphi = 0, \quad \left( \nu^{(1)} \Delta - \frac{\partial}{\partial t} \right) \psi = 0, \quad \Delta = \frac{\partial^2}{\partial x_1^2} + \frac{\partial^2}{\partial x_2^2}, \tag{7}$$

In (7)  $\nu^{(1)}$  is the kinematic viscosity, i.e.,  $\nu^{(1)} = \mu^{(1)} / \rho_0^{(1)}$ .

Supposing that  $p^{(1)} = -(T_{11} + T_{22} + T_{33})/3$ , we obtain from the constitutive relations in (5) that

$$\lambda^{(1)} = -\frac{2}{3} \mu^{(1)}. \tag{8}$$

Thus, the complete system of Eqs. (5)-(8) describe the flow of the compressible viscous fluid. Now we consider the formulation of the boundary, compatibility and impermeability conditions.

According to the foregoing discussions, on the upper face plane of the plate it must be satisfied the following boundary conditions

$$\sigma_{21}|_{x_2=0} = 0, \quad \sigma_{22}|_{x_2=0} = -P_0\delta(x_1 - Vt). \quad (9)$$

It is assumed the satisfying the compatibility conditions

$$\begin{aligned} \frac{\partial u_1}{\partial t}\Big|_{x_2=-h} &= V_1\Big|_{x_2=-h}, \quad \frac{\partial u_2}{\partial t}\Big|_{x_2=-h} = V_2\Big|_{x_2=-h}, \\ \sigma_{21}\Big|_{x_2=-h} &= T_{21}\Big|_{x_2=-h}, \quad \sigma_{22}\Big|_{x_2=-h} = T_{22}\Big|_{x_2=-h}, \end{aligned} \quad (10)$$

on the interface plane between the fluid and plate.

Finally, it is also assumed the satisfying the following impermeability conditions on the rigid wall

$$V_1\Big|_{x_2=-h-h_d} = 0, \quad V_2\Big|_{x_2=-h-h_d} = 0. \quad (11)$$

This completes the formulation of the problem under consideration and it should be noted that this formulation differs from the corresponding formulation made in the paper (Akbarov and Huseynova 2019) with the second boundary condition given in (9), i.e., in the paper (Akbarov and Huseynova 2019) it was written  $e^{i\omega t}$  instead of  $\delta(x_1 - Vt)$ . Namely, this difference causes to develop the solution method with respect to the problem under consideration and to obtain the different results with respect to the fluid flow profile in the system under consideration.

### 3. Method of solution

As usual, the problems related to the moving load is solved by employing a moving coordinate system which is also employed in the paper (Akbarov and Ismailov 2015) and in other related papers listed therein and in the work (Akbarov 2018). Based on this provision, in the present paper we also use the moving coordinate system determined through the following relations.

$$x'_1 = x_1 - Vt, \quad x'_2 = x_2. \quad (12)$$

Note that below we will omit the upper prime on the new moving coordinates in (12).

Thus, rewriting the foregoing equations and relations in the new moving coordinate system we obtain that they are valid as are if it is made the replacing the operators  $\partial/\partial t$  and  $\partial^2/\partial t^2$  with the operators  $-V\partial/\partial x_1$  and  $V^2\partial^2/\partial x_1^2$  respectively.

Note that as a result of the fluid viscosity the problem under consideration the values of the sought quantities are not symmetric or asymmetric with respect to the line  $x_1=0$ , i.e., with respect to point at which the moving load acts. Therefore for solution to the present problem unlike to the problem considered in the paper (Akbarov and Huseynova 2019) for solution to which it was employed the sinus or cosines Fourier transforms we must employ to these equations the exponential Fourier transform with respect to the moving coordinate  $x_1$ .

$$f_F(s, x_2) = \int_{-\infty}^{+\infty} f(x_1, x_2)e^{-isx_1} dx_1. \quad (13)$$

Consequently, the originals of the sought values can be found through the integrals

$$\frac{1}{2\pi} \int_{-\infty}^{+\infty} \{u_{1F}; u_{2F}; \sigma_{11F}; \sigma_{12F}; \sigma_{22F}; v_{1F}; v_{2F}; T_{11F}; T_{12F}; T_{22F}\} e^{isx_1} ds. \tag{14}$$

We introduce the dimensionless coordinates and dimensionless transformation parameter

$$\bar{x}_1 = x_1/h, \quad \bar{x}_2 = x_2/h, \quad \bar{s} = sh, \tag{15}$$

before the employing the Fourier transformation (13) and upper bars in (15) are omitted in all the subsequent solution procedure.

Now we consider determination of the Fourier transforms of the sought values and begin this determination with the solution to Eqs. (1)-(4) related to the plate motion. Thus, employing the Fourier transform to these equations and doing some mathematical transforms we obtain the following ordinary differential equations for the components of the displacement vector.

$$Au_{1F} - B \frac{du_{2F}}{dx_2} + \frac{d^2u_{1F}}{dx_2^2} = 0, \quad Du_{2F} + B \frac{du_{1F}}{dx_2} + G \frac{d^2u_{2F}}{dx_2^2} = 0, \tag{16}$$

where

$$A = X^2 - s^2 a_{11} / G_{12}, \quad B = sa_{12} / G_{12} + s, \quad D = X^2 - s^2, \quad G = a_{22} / G_{12}, \\ X^2 = \omega^2 h^2 / c_2^2, \quad c_2 = \sqrt{G_{12} / \rho}. \tag{17}$$

Using the notation

$$A_0 = \frac{AG + B^2 + D}{G}, \quad B_0 = \frac{BD}{G}, \quad k_1 = \sqrt{-\frac{A_0}{2} + \sqrt{\frac{A_0^2}{4} - B_0}}, \quad k_2 = \sqrt{-\frac{A_0}{2} - \sqrt{\frac{A_0^2}{4} - B_0}}, \tag{18}$$

The solution to Eq. (16) is found as follows

$$u_{2F} = Z_1 e^{k_1 x_2} + Z_2 e^{-k_1 x_2} + Z_3 e^{k_2 x_2} + Z_4 e^{-k_2 x_2}, \\ u_{1F} = Z_1 a_1 e^{k_1 x_2} + Z_2 a_2 e^{-k_1 x_2} + Z_3 a_3 e^{k_2 x_2} + Z_4 a_4 e^{-k_2 x_2}, \tag{19}$$

where

$$a_1 = \frac{-D - Gk_1^2}{Bk_1^2}, \quad a_2 = -a_1, \quad a_3 = \frac{-D - Gk_2^2}{Bk_2^2}, \quad a_4 = -a_3. \tag{20}$$

Using expressions (19) in the Fourier transforms of Eqs. (4) and (2) the following expressions for the Fourier transformations  $\sigma_{21F}$  and  $\sigma_{22F}$  of the stresses are determined.

$$\frac{\sigma_{21F}}{G_{12}} = Z_1 (k_1 a_1 - s) e^{k_1 x_2} + Z_2 (-k_1 a_2 - s) e^{-k_1 x_2} + Z_3 (k_2 a_3 - s) e^{k_2 x_2} + Z_4 (-k_2 a_3 - s) e^{-k_2 x_2},$$

$$\frac{\sigma_{22F}}{G_{12}} = Z_1 \left( s \frac{a_{12}}{G_{12}} a_1 + k_1 \frac{a_{22}}{G_{12}} \right) e^{k_1 x_2} + Z_2 \left( s \frac{a_{12}}{G_{12}} a_2 - k_1 \frac{a_{22}}{G_{12}} \right) e^{-k_1 x_2} +$$

$$Z_3 \left( s \frac{a_{12}}{G_{12}} a_3 + k_2 \frac{a_{22}}{G_{12}} \right) e^{k_2 x_2} + Z_2 \left( s \frac{a_{12}}{G_{12}} a_4 - k_2 \frac{a_{22}}{G_{12}} \right) e^{-k_2 x_2}. \quad (21)$$

In this way we determine the Fourier transforms of the quantities related to the plate motion.

Consider also the determination of the Fourier transforms of the quantities related to the fluid flow and begin this consideration with the determination of  $\varphi_F$  and  $\psi_F$  from the Fourier transformation of the equations in (7). Taking the relation

$$\varphi_F = -sV'h^2 \tilde{\varphi}_F, \quad \psi_F = -sV'h^2 \tilde{\psi}_F \quad (22)$$

into account, it can be written that

$$\frac{d^2 \tilde{\varphi}_F}{dx_2^2} + s^2 \left( \frac{\Omega_1^2}{1 - i4s\Omega_1^2/(3N_w^2)} - 1 \right) \tilde{\varphi}_F = 0, \quad \frac{d^2 \tilde{\psi}_F}{dx_2^2} - (s^2 - isN_w^2) \tilde{\psi}_F = 0, \quad (23)$$

where

$$\Omega_1 = \frac{V'h}{a_0}, \quad N_w^2 = \frac{V'h^2}{\nu^{(1)}}. \quad (24)$$

Note that the dimensionless parameter  $\Omega_1$  in (24) characterizes the fluid compressibility, according to which, it may be considerable under high velocity of the moving load. Moreover, note that the other dimensionless parameter  $N_w$  in (24) characterizes the fluid viscosity, according to which, it may be considerable for the low velocity of the moving load and for thin plates.

Thus, using the foregoing notation and assumptions, the solutions to the equations in (23) are found as follows

$$\tilde{\varphi}_F = Z_5 e^{\delta_1 x_2} + Z_7 e^{-\delta_1 x_2}, \quad \tilde{\psi}_F = Z_6 e^{\gamma_1 x_2} + Z_8 e^{-\gamma_1 x_2}, \quad (25)$$

where

$$\delta_1 = s^2 \sqrt{1 - \frac{\Omega_1^2}{1 - i4s\Omega_1^2/(3N_w^2)}}, \quad \gamma_1 = \sqrt{s^2 - isN_w^2}. \quad (26)$$

According to (25), (26), (6) and (5) the following expressions are obtained for the Fourier transforms of the velocities, pressure and stresses.

$$\begin{aligned} V_{1F} &= -sV'h \left[ -Z_5 s e^{\delta_1 x_2} - Z_7 s e^{-\delta_1 x_2} + Z_6 e^{\gamma_1 x_2} + Z_8 e^{-\gamma_1 x_2} \right], \\ V_{2F} &= -sV'h \left[ Z_5 \delta_1 e^{\delta_1 x_2} - Z_7 \delta_1 e^{-\delta_1 x_2} - Z_6 s e^{\gamma_1 x_2} - Z_8 s e^{-\gamma_1 x_2} \right], \\ T_{22F} &= \mu^{(1)} (-sV') \left[ Z_5 \left( \frac{4}{3} \delta_1^2 + \frac{2}{3} s^2 - R_0 \right) e^{\delta_1 x_2} + Z_7 \left( \frac{4}{3} \delta_1^2 + \frac{2}{3} s^2 - R_0 \right) e^{-\delta_1 x_2} + \right. \\ &\quad \left. Z_6 \left( -s\gamma_1 - \frac{2}{3} s\gamma_1 \right) e^{\gamma_1 x_2} + Z_8 \left( s\gamma_1 + \frac{2}{3} s\gamma_1 \right) e^{-\gamma_1 x_2} \right], \end{aligned}$$

$$T_{21F} = -\mu^{(1)}(-sV') \left[ 2s\delta_1 Z_5 e^{\delta_1 x_2} - 2s\delta_1 Z_7 e^{-\delta_1 x_2} + (s^2 + \gamma_1^2) Z_6 e^{\gamma_1 x_2} + (s^2 + \gamma_1^2) Z_8 e^{-\gamma_1 x_2} \right],$$

$$p_F^{(1)} = \mu^{(1)}(-sV') R_0 \left( Z_5 e^{\delta_1 x_2} + Z_7 e^{-\delta_1 x_2} \right), \quad (27)$$

where

$$R_0 = -\frac{4}{3} \frac{s^2 \Omega_1^2}{1 - i4s\Omega_1^2 / (3N_w^2)} + isN_w^2. \quad (28)$$

Finally, the following system of equations with respect to the unknowns  $Z_1, Z_2, \dots, Z_8$  which enter the expressions of the Fourier transforms of the sought values in (19), (21) and (27) are obtained from the boundary conditions in (9), the compatibility conditions in (10) and impermeability conditions in (11).

$$\begin{aligned} (\sigma_{21F}/G_{12})|_{x_2=0} &= Z_1\alpha_{11} + Z_2\alpha_{12} + Z_3\alpha_{13} + Z_4\alpha_{14} = 0, \\ (\sigma_{22F}/G_{12})|_{x_2=0} &= Z_1\alpha_{21} + Z_2\alpha_{22} + Z_3\alpha_{23} + Z_4\alpha_{24} = -P_0/G_{12}, \\ \frac{\partial u_{1F}}{\partial t} \Big|_{x_2=-h} - V_{1F}|_{x_2=-h} &= i\omega(Z_1\alpha_{31} + Z_2\alpha_{32} + Z_3\alpha_{33} + Z_4\alpha_{34}) - \\ &\omega h(Z_5\alpha_{35} + Z_6\alpha_{36} + Z_7\alpha_{37} + Z_8\alpha_{38}) = 0, \\ \frac{\partial u_{2F}}{\partial t} \Big|_{x_2=-h} - V_{2F}|_{x_2=-h} &= i\omega(Z_1\alpha_{41} + Z_2\alpha_{42} + Z_3\alpha_{43} + Z_4\alpha_{44}) - \\ &\omega h(Z_5\alpha_{45} + Z_6\alpha_{46} + Z_7\alpha_{47} + Z_8\alpha_{48}) = 0, \\ (\sigma_{21}/G_{12})|_{x_2=-h} - (T_{21}/G_{12})|_{x_2=-h} &= Z_1\alpha_{51} + Z_2\alpha_{52} + Z_3\alpha_{53} + Z_4\alpha_{54} - \\ &M(Z_5\alpha_{55} + Z_6\alpha_{56} + Z_7\alpha_{57} + Z_8\alpha_{58}) = 0, \\ (\sigma_{22}/G_{12})|_{x_2=-h} - (T_{22}/G_{12})|_{x_2=-h} &= Z_1\alpha_{61} + Z_2\alpha_{62} + Z_3\alpha_{63} + Z_4\alpha_{64} - \\ &M(Z_5\alpha_{65} + Z_6\alpha_{66} + Z_7\alpha_{67} + Z_8\alpha_{68}) = 0, \\ V_{1F}|_{x_2=-h-h_d} &= \omega h(Z_5\alpha_{75} + Z_6\alpha_{76} + Z_7\alpha_{77} + Z_8\alpha_{78}) = 0, \\ V_{2F}|_{x_2=-h-h_d} &= \omega h(Z_5\alpha_{85} + Z_6\alpha_{86} + Z_7\alpha_{87} + Z_8\alpha_{88}) = 0 \end{aligned} \quad (29)$$

where

$$M = \frac{\mu^{(1)}V'}{G_{12}}. \quad (30)$$

It is not given here the expressions of the coefficients  $\alpha_{nm}$  ( $n,m=1,2,\dots,8$ ) in (29) because they may be easily determined from Eqs. (19), (21) and (27).

Thus, we determine the unknown constants  $Z_1, Z_2, \dots, Z_8$  as follows

$$Z_k = \frac{\det \|\beta_{nm}^k\|}{\det \|\alpha_{nm}\|}, \quad k=1,2,\dots,8, \quad (31)$$

where the matrix  $(\beta_{nm}^k)$  is obtained from the matrix  $(\alpha_{nm})$  by replacing the  $k$ -th column of the latter with the column  $(0, -P_0 / G_{12}, 0, 0, 0, 0, 0, 0)^T$ .

Now we consider the algorithm which is used under calculation of the integrals in (14) and for this purpose, firstly we note the following reasoning. If we take the Fourier transformation parameter  $s$  as the wavenumber, then the equation

$$\det \|\alpha_{nm}\| = 0, \quad n; m = 1, 2, \dots, 8, \quad (32)$$

coincides with the dispersion equation of the waves with the velocity  $V$  propagated in the direction of the  $Ox_1$  axis in the system under consideration. Therefore, Eq. (32) must have complex roots only with respect to the  $s$  for the system under consideration and this is caused by the viscosity of the fluid. However, as usual, the viscosity of the Newtonian fluids is insignificant in the quantitative sense and therefore in some cases within the scope of the PC calculation accuracy, the Eq. (32) may have “real roots” under which the integrated expressions in (14) have singularity.

In such cases the corresponding calculation algorithm was discussed in monograph (Akbarov 2015) and other works listed in this monograph. According to this algorithm, in the mentioned cases the wavenumber integrals (14) may be evaluated along the Sommerfeld contour examples for which is shown in the monograph (Akbarov 2015).

Fortunately, in the present investigations under calculation of the integrals in (14) the aforementioned “real roots” do not appear and according to expression in (14), the sought values are determined through the following relation:

$$\begin{aligned} \{u_1; u_2; \sigma_{11}; \sigma_{12}; \sigma_{22}; v_1; v_2; T_{11}; T_{12}; T_{22}\} = \frac{1}{2\pi} \operatorname{Re} \left[ \int_{-\infty}^{+\infty} \{u_{1F}; u_{2F}; \sigma_{11F}; \right. \\ \left. \sigma_{12F}; \sigma_{22F}; v_{1F}; v_{2F}; T_{11F}; T_{12F}; T_{22F}\} e^{isx_1} ds \right]. \end{aligned} \quad (32)$$

Note that under calculation procedures, the improper integrals  $\int_{-\infty}^{+\infty} f(s) \cos(sx_1) ds$  and  $\int_{-\infty}^{-\infty} f(s) \sin(sx_1) ds$  which follows from (32) are replaced by the corresponding definite integrals  $\int_{-S_1^*}^{+S_1^*} f(s) \cos(sx_1) ds$  and  $\int_{-S_1^*}^{+S_1^*} f(s) \sin(sx_1) ds$ , respectively. The values of  $S_1^*$  are determined from the convergence requirement of the numerical results.

Under calculation of the mentioned definite integrals, the integration interval  $[-S_1^*, +S_1^*]$  is further divided into a certain number of shorter intervals, which are used in the Gauss integration algorithm. The values of the integrated expressions at the sample points are calculated through the Eqs. (19), (21) and (27). All these procedures are performed automatically with the PC programs constructed by the authors in MATLAB.

This completes the consideration of the method of solution to the problem under consideration.

#### 4. Numerical results and discussions

For numerical investigation we assume that the fluid is Glycerin with viscosity coefficient  $\mu^{(1)}=1.393 \text{ kg/m}\cdot\text{s}$ , density  $\rho_0^{(1)}=1260 \text{ kg/m}^3$  and sound speed  $a_0=1927 \text{ m/s}$  (Guz 2009). As in the paper (Akbarov and Huseynova 2019), the parameters  $k_1$  and  $k_2$  determined as

$$\rho/\rho_0^{(1)} = k_1, c_2/a_0 = k_2, G_{12} = (c_2)^2 \rho \quad (32)$$

are introduced for determination the density and shear modulus of elasticity in the  $Ox_1x_2$  plane of the plate material through the mechanical properties of the fluid. Consequently, if we know the density of the fluid, then giving the values for the  $k_1$  we determine the density of the plate material, as well as if we know the sound speed in the fluid, then giving the values for the  $k_2$  we determine the values for the shear modulus  $G_{12}$

Thus, selecting the values for the constants  $k_1$  and  $k_2$  we determine the density and shear modulus of the plate material through the density and sound speed of the fluid material, and an increase in the values of the  $k_1$  (of the  $k_2$ ) means an increase in the values of the density (of the shear modulus) of the plate material and under fixed value of the fluid density (under fixed sound speed in the fluid). Moreover, we use the following ratios which characterize the anisotropy of the plate material.

$$E_1 / G_{12}, E_1 / E_2, E_2 / E_3, E_1 / E_3, \quad (33)$$

and assume that

$$\nu_{12} = \nu_{13} = \nu_{23} = 0.3, \quad \nu_{21} = \nu_{12} \frac{E_1}{E_2}, \quad \nu_{31} = \nu_{13} \frac{E_1}{E_3}, \quad \nu_{32} = \nu_{23} \frac{E_2}{E_3}. \quad (34)$$

At the same time, we assume that

$$E_2 = E_3, \quad E_1 / E_2 = 1.5 \quad (35)$$

In this way through the ratio  $E_1/G_{12}$  we can characterize the influence of the anisotropy of the plate material on the fluid flow profile which is the main aim of the present numerical investigations. Consequently, in the present paper we will consider the numerical results illustrating the influence of the  $V/h, x_1/h, h_d/h, E_1/G_{12}, k_1$  and  $k_2$  on the fluid flow profile which is caused as result of the moving load action on the plate which is in contact with fluid and we assume that  $h=0.001 \text{ m}$ .

Note that, according to the convergence investigations carried out in the paper (Akbarov and Ismailov 2017), under obtaining numerical results it is assumed that  $S_1^* = 9$  the interval  $[-S_1^*, S_1^*]$  is divided into 4000 shorter subintervals in each of which it is used the Gauss integration algorithm with ten sample points.

The convergence of the numerical results in the selected numbers of the subintervals and in the selected length of the integration interval was illustrated not only in the papers (Akbarov and Ismailov 2016, 2017 and 2018) and in others listed therein. Therefore, the convergence of the numerical results doesn't analyzed here. The trustiness of the used PC programs which are used under obtaining the numerical results is also used under obtaining of the numerical results given in the paper (Akbarov and Huseynova 2019) tested with obtaining in the particular cases the known results and with agreeing the obtained results with the physico-mechanical considerations. We do not consider here examples for such testing and begin to analyze the numerical results illustrated the fluid flow profile in the system under consideration.

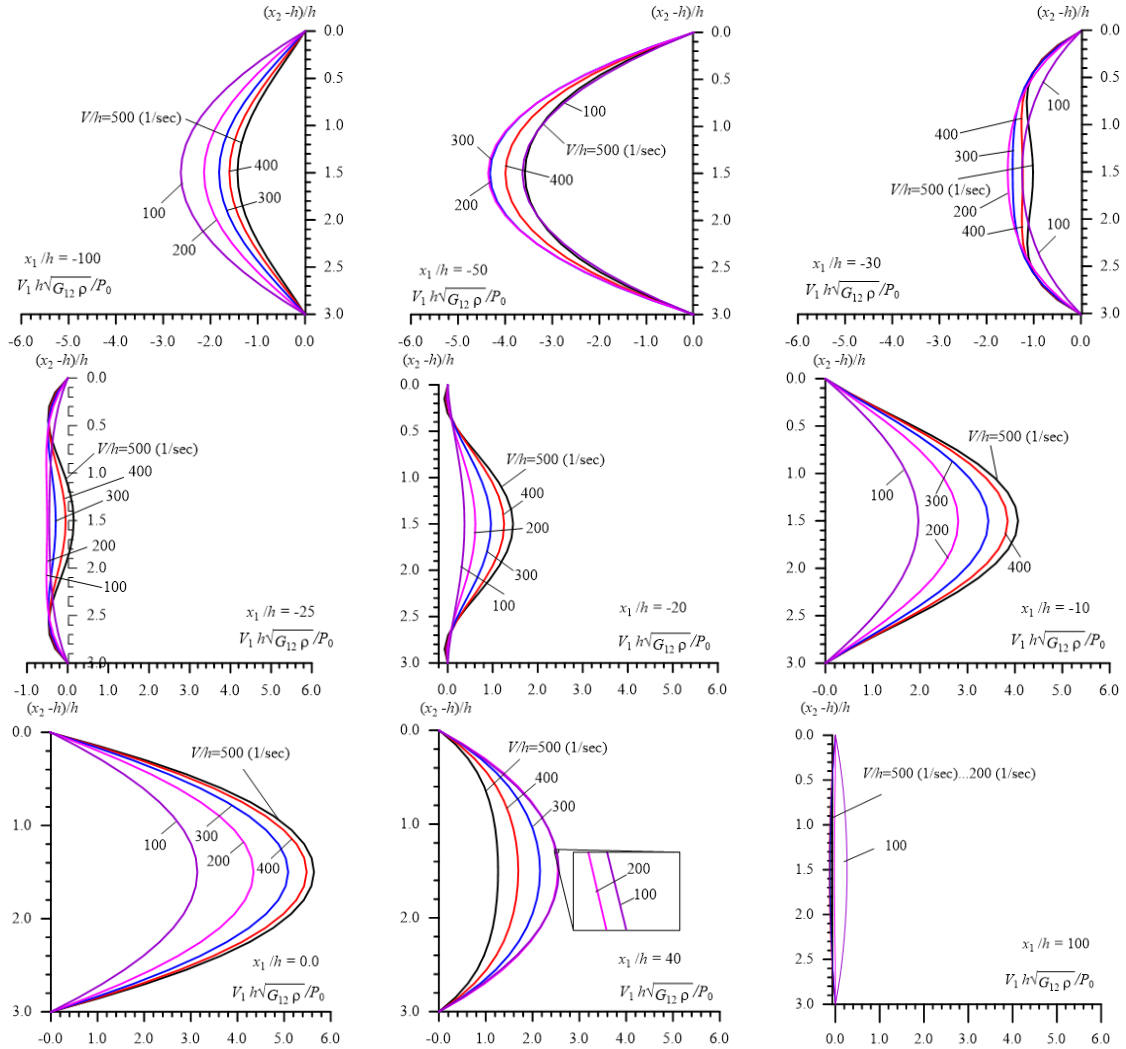


Fig. 2 Fluid flow profile in the  $Ox_1$  axis direction obtained for various moving load velocity  $V/h$  and in various distance  $x_1/h$  from the moving load in the case where  $E_1/G_{12}=3$  and  $h_d/h=3$

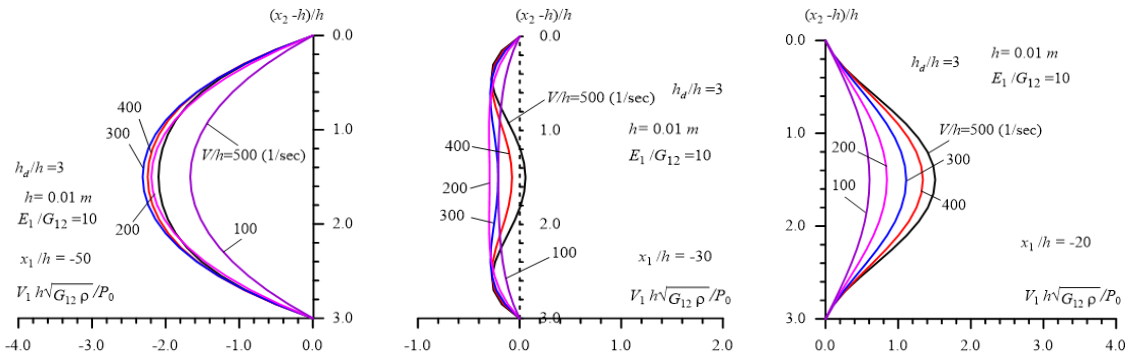


Fig. 3 Fluid flow profile in the  $Ox_1$  axis direction obtained for various moving load velocity  $V/h$  and in various distance  $x_1/h$  from the moving load in the case where  $E_1/G_{12}=10$  and  $h_d/h=3$

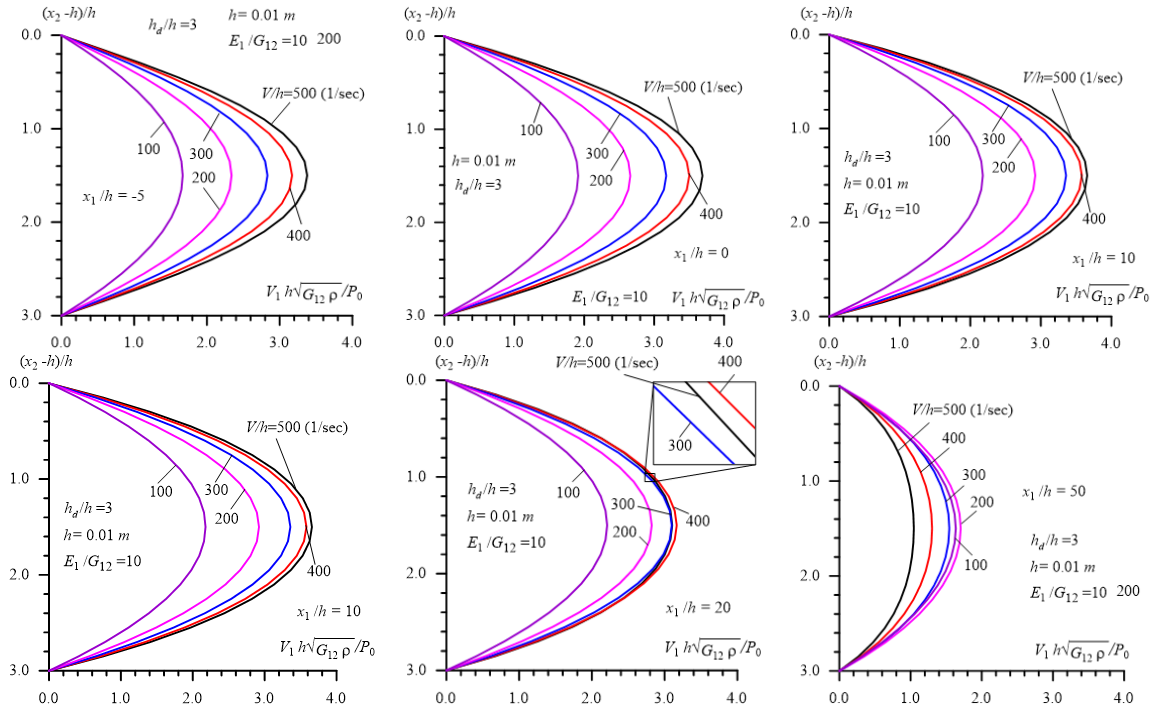


Fig. 3 Continued

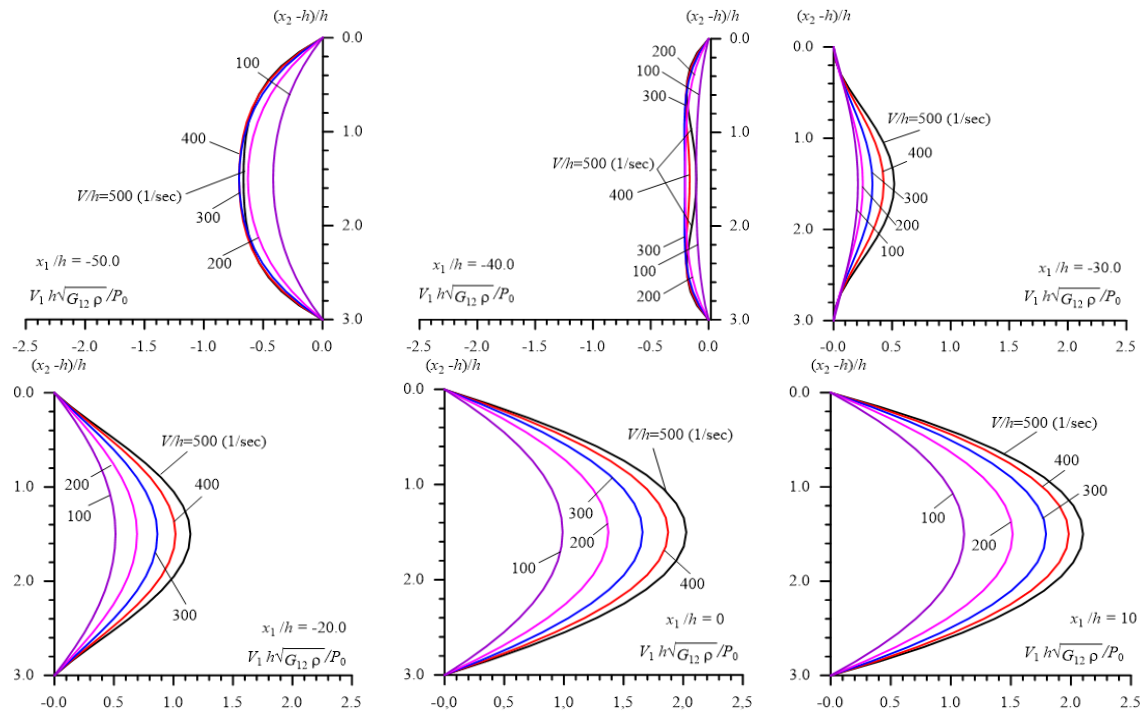


Fig. 4 Fluid flow profile in the  $Ox_1$  axis direction obtained for various moving load velocity  $V/h$  and in various distance  $x_1/h$  from the moving load in the case where  $E_1/G_{12}=50$  and  $h_d/h=3$

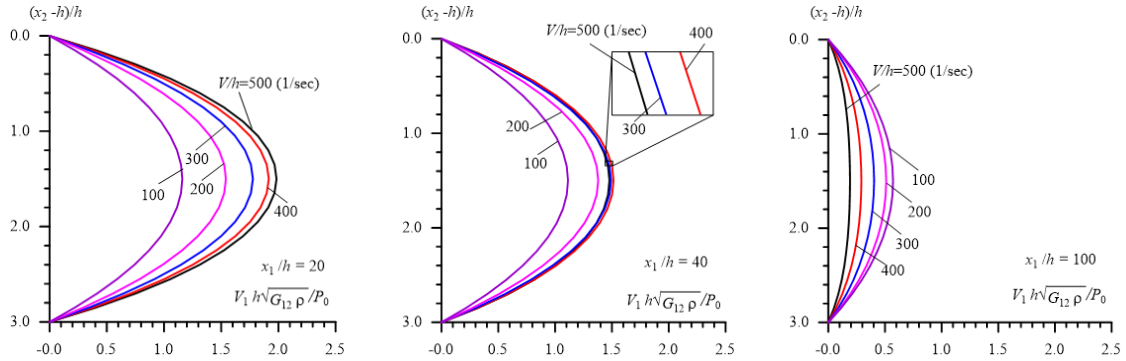


Fig. 4 Continued

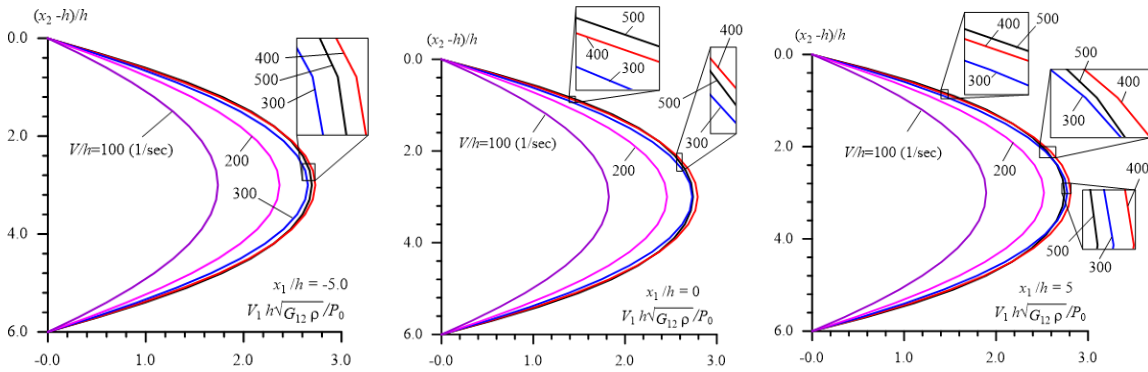


Fig. 5 Fluid flow profile in the  $Ox_1$  axis direction obtained for various moving load velocity  $V/h$  and in various distance  $x_1/h$  from the moving load in the case where  $E_1/G_{12}=50$  and  $h_d/h=6$

Thus, we consider the graphs given in Figs. 2, 3 and 4 which show the distribution of the dimensionless fluid flow velocity  $V_1 h \sqrt{G_{12} \rho} / P_0$  with respect to  $(x_2 - h) / h$  (along the fluid depth) in the cases where  $E_1 / G_{12} = 3, 10$  and  $50$ , respectively for various values of the load moving velocity  $V/h$  and for various distance in behind and in ahead from the point at which the moving load acts (i.e., for various values of  $x_1/h$ ) under  $h_d/d=3$ . Note that these results are obtained in the case where  $k_1=k_2=1$  which introduced through the relations in (32).

It follows from the observation of the results given in Figs. 2, 3 and 4 that the fluid flow profile in the case under consideration in the near vicinity at the point at which the moving load acts is similar to the well-known Poiseuille flow between two plates. However, it also follows from these results that the mentioned similarity is violated with the distance from the moving load acting point, especially in behind of the moving load. Moreover, in behind of the moving load at a certain distance from that, the fluid flow velocity in the  $Ox_1$  axis direction changes its flow direction, i.e., fluid flow direction becomes vice-versa to this axis direction. This “certain distance” for the cases  $E_1 / G_{12} = 3, 10$  and  $50$  can be taken approximately as  $x_1 / h = (x_1 / h)^* \approx -25, -30$  and  $-10$ . Namely, around these points, the fluid flow profile differs significantly from the Poiseuille flow and becomes complicated and in the cases where  $x_1/h < (x_1/h)^*$  the fluid flow direction is vice-versa to that which is observed in the near vicinity of the cross-sections of the fluid-strip which are near to the point at which the moving load act. The comparison of the results illustrated in Figs. 2, 3 and 4 with each

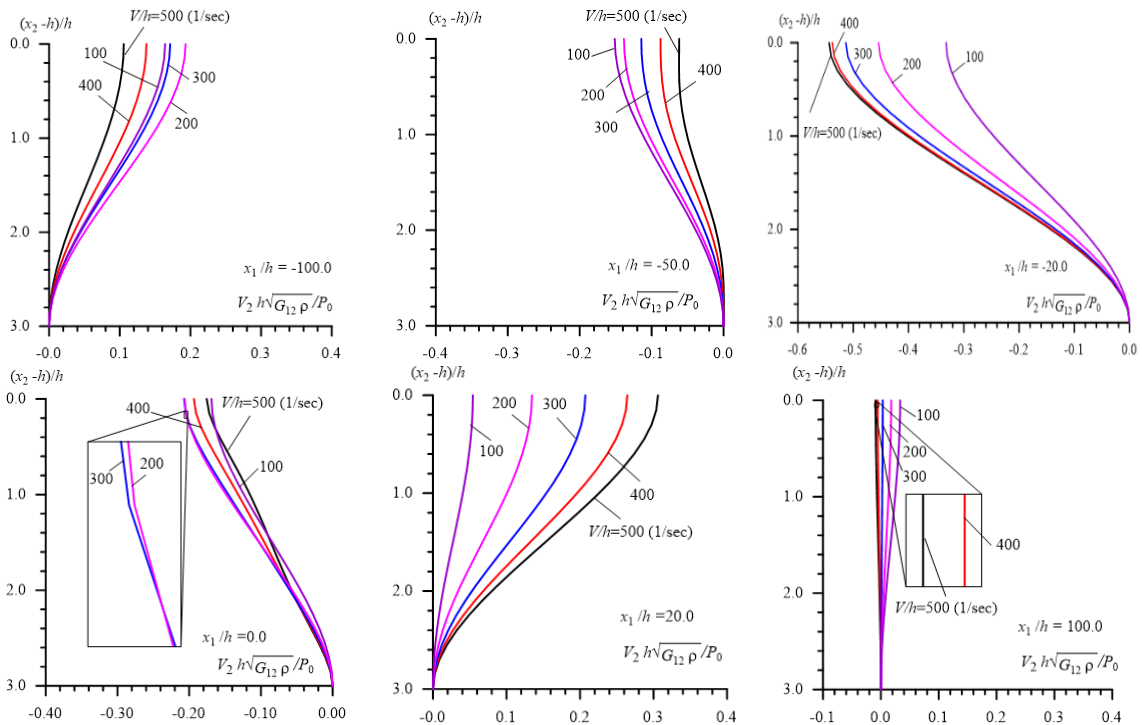


Fig. 6 Fluid flow profile in the  $Ox_2$  axis direction obtained for various moving load velocity  $V/h$  and in various distance  $x_1/h$  from the moving load in the case where  $E_1/G_{12}=3$  and  $h_d/h=3$

other shows that the increase in the values of the ratio  $E_1/G_{12}$  (i.e., the decrease of the plate stiffness with respect to the shear deformation) causes, in general, to decrease of the fluid flow velocity. Moreover, analyze the results obtained for various values of the moving load velocity shows that in the near vicinity of the moving load an increase in the values  $V/h$  causes an increase of the fluid flow velocity. However, after a certain distance from the moving load, this conclusion is violated and the character of the influence of the  $V/h$  on the fluid flow velocity depends on the mentioned distance.

Note that the foregoing results are obtained only for the case where  $h_d/d=3$  which characterizes the influence of the fluid's depth on the fluid flow profiles under consideration. The study of the change the ratio  $h_d/d$  on the fluid flow profile is also one of interesting fact which requires the detail investigations. However, here we do not consider this question in detail and as an example for such influence in Fig. 5 it is given some results related to the fluid flow profile obtained in the case where  $h_d/d=6$  under  $E_1/G_{12}=50$ . The comparison of the results given in Fig. 5 with corresponding ones given in Fig. 4 shows that an increase in the value of the ratio  $h_d/d$  causes to decrease of the absolute maximum value of the fluid flow velocity in the  $Ox_1$  axis direction.

Besides all of these, it should be noted that, according to the problem geometry and to the external load location, the fluid flow profile must be non-symmetric with respect to the middle plane of the fluid-strip, i.e., with respect to the  $x_2=(h_d-h)/2$ . However, the observation of the obtained results do not show clearly such non-symmetry, most likely these profiles are similar to the symmetric fluid flow profile with respect to the indicated plane. In fact, the detail analyses of the numerical data, according to which the graphs given in Figs. 2, 3 and 4 are constructed, shows that there are the mentioned non symmetry with respect to the plane  $x_2=(h_d-h)/2$ . However, the difference

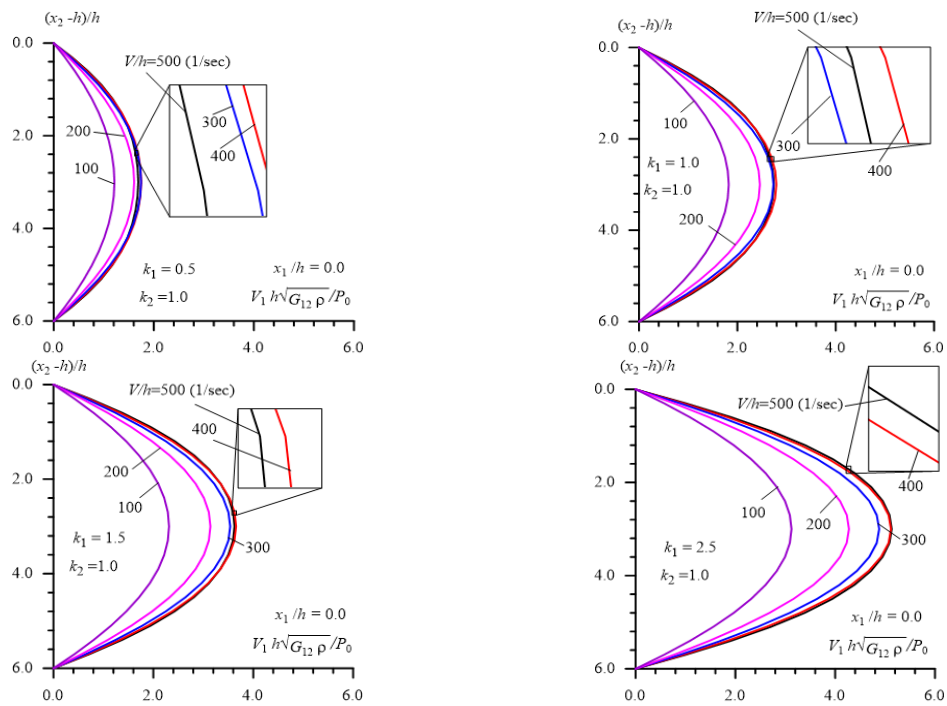


Fig. 7 The influence of the parameter  $k_1$  on the fluid flow profile in  $Ox_1$  direction obtained for various moving load velocity  $V/h$  and in various distance  $x_1/h$  from the moving load in the case where  $E_1/G_{12}=50$  and  $h_d/h=6$

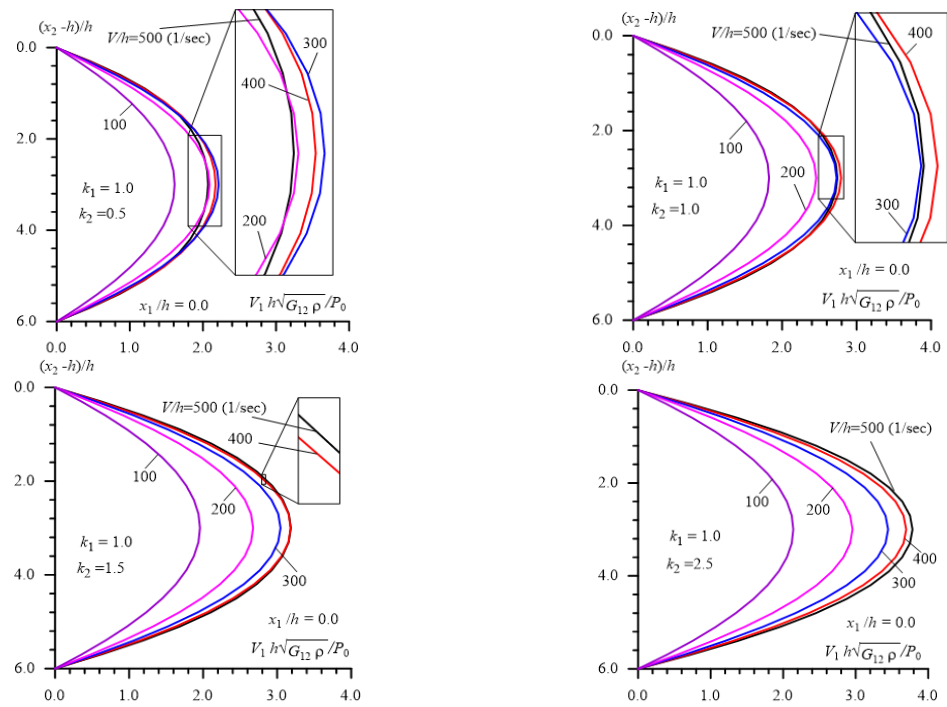


Fig. 8 The influence of the parameter  $k_2$  on the fluid flow profile in  $Ox_1$  direction obtained for various moving load velocity  $V/h$  and in various distance  $x_1/h$  from the moving load in the case where  $E_1/G_{12}=50$  and  $h_d/h=6$

between the values of the  $V_1$  velocity obtained at the points which have the symmetric location with respect to the plane  $x_2=(h_d-h)/2$  so few that the above-noted non-symmetry doesn't observed in the graphs given in Figs. 2, 3 and 4. At the same time, the non-symmetry character of the quantities related to the fluid flow clearly observed on the graphs related to the  $V_2$  velocity of the fluid. These graphs are given in Fig. 6 which are constructed in the case where  $E_1/G_{12}=3$  and  $h_d/h=3$  for various moving load velocity  $V/h$  and in various distance from the load location point.

In Figs. 1, 2, 3, 4 and 5 it is clearly observed the non-symmetry of the profiles of the fluid flow with respect to the point at which the moving load acts, i.e. with respect to the point  $x_1/h=0$ . It should be noted that this non symmetry is caused with the fluid viscosity which is also observed in the paper (Akbarov and Ismailov 2015).

Note that all the foregoing results are obtained in the case where  $k_1=k_2=1$ , i.e., in the case where the density of the plate material is equal to the fluid density and the sound speed in the fluid is equal to the shear wave propagation velocity in the plate material. Now we consider the results illustrated the influence of the parameters  $k_1$  and  $k_2$  on the fluid flow profile. The results illustrated this influence are given in Figs. 7 and 8 which are obtained for the various values of the  $k_1$  (under  $k_2=1$ ) and for various values of  $k_2$  (under  $k_1=1$ ) respectively. It follows from the analyses of the results given in Fig. 7 that an increase in the plate material density causes to increase fluid flow velocity in the load moving direction. As well as, it follows from the analyses of the results given in Fig. 8 that an increase of the shear wave velocity in the plate material also causes to increase the fluid flow velocity in the  $Ox_1$  axis direction.

It is known that fluid flow and its flow direction is caused by the pressure gradient and if the projection of this gradient along the  $Ox_1$  axis is negative then the fluid flow direction must be coincide with the  $Ox_1$  axis direction, otherwise the fluid flow direction must be against with the  $Ox_1$  axis direction. In connection with this, we consider the values of the pressure in the various cross section in the fluid strip which are illustrated with the graphs given in Fig. 9 obtained in the case where  $V/h=500$  (1/sec),  $E_1/G_{12}=3$  and  $h_d/h=3$ . Moreover, in Fig. 10 in the same case it is shown the graphs of the pressure distribution along the fluid strip thickness at the various distance from the moving load. It follows from these results that the values of the pressure can be taken as constant

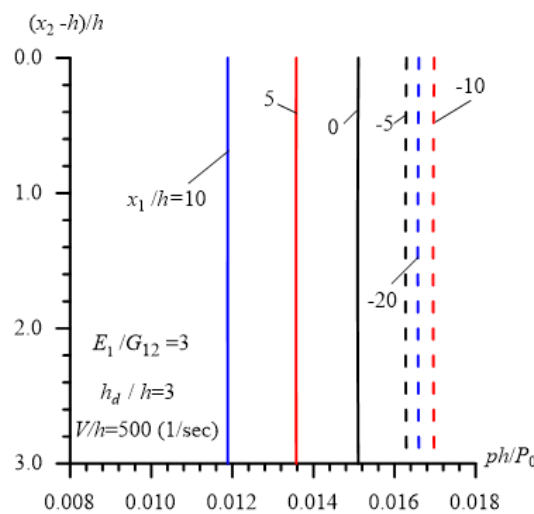


Fig. 9 The values of the pressure in various cross section of the fluid strip

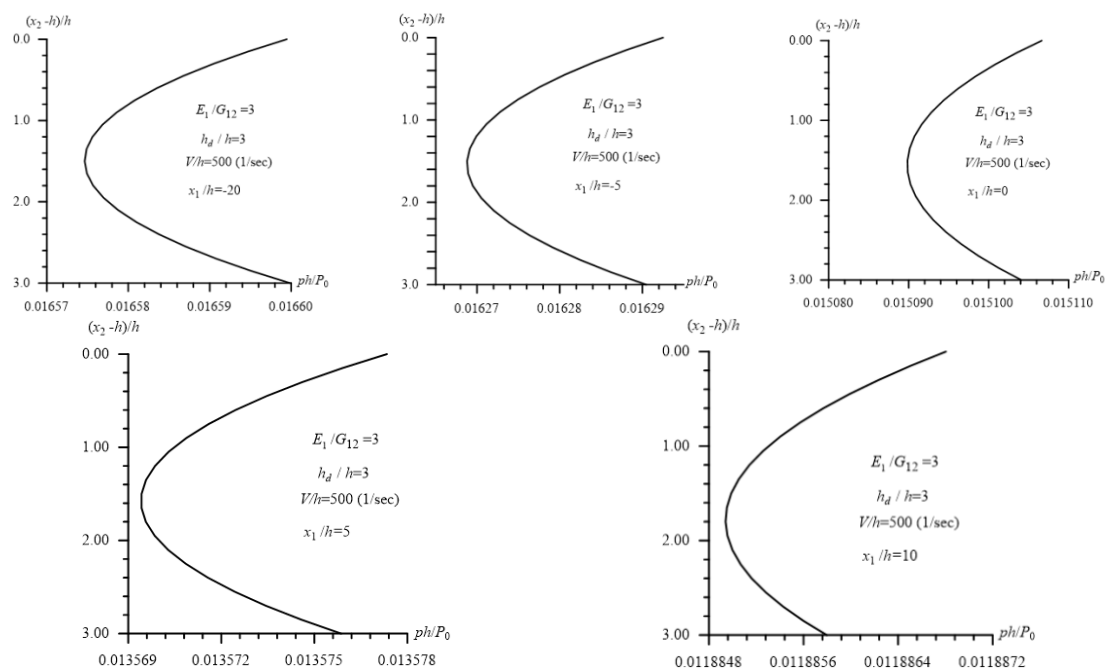


Fig. 10 The distribution of the pressure along the fluid strip thickness

along the thickness of the fluid strip thickness with accuracy  $10^{-4}$ . However, the values of the pressure depends significantly not only on the distance from the point at which the moving load acts but also on the moving load velocity. Consequently the graphs given above on the fluid flow profiles illustrate also a certain information on the distribution of the pressure gradient in this fluid which appear as a result of the action of the moving load acting on the plate which is in contact with the fluid.

This completes the analyses of the numerical results.

## 5. Conclusions

Thus, the present paper studies the fluid flow profile in the system consisting of the orthotropic plate, compressible (barotropic) viscous fluid and rigid wall in the case where on the upper face plane of the plate the moving load acts. The plane-strain state in the plate and the plane flow in the fluid is considered. The motion of the plate is described within the scope of the exact equations and relations of the elastodynamics for anisotropic bodies and the fluid flow is described by the linearized Navier-Stokes equations. Numerical results are presented on the fluid flow profiles and on the influence of the problem parameters such as an anisotropy of the plate material, load moving velocity, fluid depth, the plate material density and shear wave propagation velocity are presented and discussed for the case where the fluid is Glycerin.

According to these results it is established the following concrete conclusions:

- In the near vicinity of the moving load in the ahead and in the behind of this load the fluid flow profile is similar to the corresponding Poiseuille flow profile.

- The amplitude of this profile decrease with the distance from the point at which this load acts.
- In the direction which coincides with the load moving direction the form of this profile remain same with the distance from the moving load. However, in the direction which is against to the load moving direction the form of the fluid flow profile change significantly with the distance from the moving load and after a certain distance the fluid flows in the direction which is against with moving load direction.
- An increase in the values of the ratio  $E_1/G_{12}$  (i.e., a decrease in the shear modulus of the plate material) causes to decrease of the amplitude of the fluid flow profile.
- An increase of the plate material density and as well as an increase of the shear wave propagation velocity of this material causes to increase the fluid flow velocity along the moving load direction.

The results obtained in the present paper allows us to get the theoretical base for creating and controlling the fluid flow through the moving load acting on the plate which is in contact with the fluid.

## References

- Akbarov, S.D. (2015), *Dynamics of Pre-strained Bi-material Elastic Systems: Linearized Three-Dimensional Approach*, Springer, New York, USA.
- Akbarov, S.D. (2018), “Forced vibration of the hydro-viscoelastic and-elastic systems consisting of the viscoelastic or elastic plate, compressible viscous fluid and rigid wall: a review”, *Appl. Comput. Math.*, **17**(3), 221-245.
- Akbarov, S.D. and Huseynova, T.V. (2019), “Forced vibration of the hydro-elastic system consisting of the orthotropic plate, compressible viscous fluid and rigid wall”, *Coupl. Syst. Mech.*, **8**(3), 199-218. <https://doi.org/10.12989/csm.2019.8.3.199>.
- Akbarov, S.D. and Ismailov, M.I. (2014), “Forced vibration of a system consisting of a pre-strained highly elastic plate under compressible viscous fluid loading”, *CMES: Comput. Model. Eng. Sci.*, **97**(4), 359-390. <https://doi.org/10.3970/cmcs.2014.097.359>.
- Akbarov, S.D. and Ismailov, M.I. (2015), “Dynamics of the moving load acting on the hydro-elastic system consisting of the elastic plate, compressible viscous fluid and rigid wall”, *CMC: Comput. Mater. Continua*, **45**(2), 75-10. <https://doi.org/10.3970/cmc.2015.045.075>.
- Akbarov, S.D. and Ismailov, M.I. (2016), “Frequency response of a pre-stressed metal elastic plate under compressible viscous fluid loading”, *Appl. Comput. Math.*, **15**(2), 172-188.
- Akbarov, S.D. and Ismailov, M.I. (2017), “The forced vibration of the system consisting of an elastic plate, compressible viscous fluid and rigid wall”, *J. Vib. Control*, **23**(11), 1809-1827. <https://doi.org/10.1177/1077546315601299>.
- Akbarov, S.D. and Ismailov, M.I. (2018), “The influence of the rheological parameters of a hydro-viscoelastic system consisting of a viscoelastic plate, viscous fluid and rigid wall on the frequency response of this system”, *J. Vib. Control*, **24**(7), 1341-1363. <https://doi.org/10.1177/1077546316660029>.
- Akbarov, S.D. and Panakhli, P.G. (2017), “On the particularities of the forced vibration of the hydro-elastic system consisting of a moving elastic plate, compressible viscous fluid and rigid wall”, *Coupl. Syst. Mech.*, **6**(3), 287-316. <https://doi.org/10.12989/csm.2017.6.3.287>.
- Akbarov, S.D., Ismailov, M.I. and Aliyev, S.A. (2017) “The influence of the initial strains of the highly elastic plate on the forced vibration of the hydro-elastic system consisting of this plate, compressible viscous fluid, and rigid wall”, *Coupl. Syst. Mech.*, **6**(4), 287-316. <https://doi.org/10.12989/csm.2017.6.4.439>.
- Amabili, M. (1996), “Effect of finite fluid depth on the hydroelastic vibrations of circular and annular plates”, *J. Sound Vib.*, **193**, 909-925. <https://doi.org/10.1006/jsvi.1996.0322>.
- Amabili, M. and Kwak, M.K. (1996), “Free vibrations of circular plates coupled with liquids: revising the

- Lamb problem”, *J. Fluid. Struct.*, **7**, 743-761. <https://doi.org/10.1006/jfls.1996.0051>.
- Atkinson, C. and Manrique de Lara, M. (2007), “The frequency response of a rectangular cantilever plate vibrating in a viscous fluid”, *J. Sound Vib.*, **300**, 352-367. <https://doi.org/10.1016/j.jsv.2006.08.011>.
- Bagno, A.M. (2015), “The dispersion spectrum of wave process in a system consisting of an ideal fluid layer and compressible elastic layer”, *Int. Appl. Mech.*, **51**(6), 52-60. <https://doi.org/10.1007/s10778-015-0721-7>.
- Bagno, A.M. and Guz, A.N. (1997), “Elastic waves in prestressed bodies interacting with fluid (Survey)”, *Int. Appl. Mech.*, **33**(6), 435-465. <https://doi.org/10.1007/BF02700652>.
- Bagno, A.M., Guz, A.N. and Shchuruk, G.I. (1994), “Influence of fluid viscosity on waves in an initially deformed compressible elastic layer interacting with a fluid medium”, *Int. Appl. Mech.*, **30**(9), 643-649. <https://doi.org/10.1007/BF00847075>.
- Das, H.N. and Kapuria, S. (2016), “On the use of bend-twist coupling in full-scale composite marine propellers for improving hydrodynamic performance”, *J. Fluid. Struct.*, **61**, 132-153. <https://doi.org/10.1016/j.jfluidstructs.2015.11.008>.
- Fu, S., Cui, W., Chen, X. and Wang, C. (2005), “Hydroelastic analysis of a nonlinearity connected floating bridge subjected to moving loads”, *Marine Struct.*, **18**, 85-107. <https://doi.org/10.1016/j.marstruc.2005.05.001>.
- Gagani, A.I. and Echtermeyer, A.T. (2019), “Influence of delaminations on fluid diffusion in multidirectional composite laminates-Theory and experiments”, *Int. J. Solid. Struct.*, **158**, 232-242. <https://doi.org/10.1016/j.ijsolstr.2018.09.009>.
- Guz, A.N. (2009), *Dynamics of Compressible Viscous Fluid*, Cambridge Scientific Publishers.
- Guz, A.N., Zhuk, A.P. and Bagno, A.M. (2016), “Dynamics of elastic bodies, solid particles, and fluid parcels in a compressible viscous fluid (Review)”, *Int. Appl. Mech.*, **52**(5), 449-507. <https://doi.org/10.1007/s10778-016-0770-6>.
- Hadzalic, E., Ibrahimbegovic, A. and Dolarevic, S. (2018), “Fluid-structure interaction system predicting both internal pore pressure and outside hydrodynamic pressure”, *Coupl. Syst. Mech.*, **7**(6), 649-668. <https://doi.org/10.12989/csm.2018.7.6.649>.
- Jeong, K.H. and Kim, K.J. (2005), “Hydroelastic vibration of a circular plate submerged in a bounded compressible fluid”, *J. Sound Vib.*, **283**, 153-172. <https://doi.org/10.1016/j.jsv.2004.04.029>.
- Kaneko, S., Hong, G., Mitsume, N., Yamada, T. and Yoshimura, S. (2018), “Numerical study of active control by piezoelectric materials for fluid-structure interaction problems”, *J. Sound Vib.*, **435**, 23-35. <https://doi.org/10.1016/j.jsv.2018.07.044>.
- Kelvani, A., Shooshtar, A. and Sani, A.A. (2013), “A closed form solution for fluid structure system: Shear-beam-compressible fluid”, *Coupl. Syst. Mech.*, **2**(2), 127-146. <https://doi.org/10.12989/csm.2013.2.2.127>.
- Kozlovsky, Y. (2009), “Vibration of plates in contact with viscous fluid: Extension of Lamb’s model”, *J. Sound Vib.*, **326**, 332-339. <https://doi.org/10.1016/j.jsv.2009.04.031>.
- Kwak, H. and Kim, K. (1991), “Axisymmetric vibration of circular plates in contact with water”, *J. Sound Vib.*, **146**, 381-216. [https://doi.org/10.1016/0022-460X\(91\)90696-H](https://doi.org/10.1016/0022-460X(91)90696-H).
- Kwak, M.K. (1997), “Hydroelastic vibration of circular plates (Fourier-Bessel series approach)”, *J. Sound Vib.*, **201**, 293-303. <https://doi.org/10.1006/jsvi.1996.0775>.
- Kwak, M.K. and Han, S.B. (2000), “Effect of fluid depth on the hydroelastic vibration of free-edge circular plate”, *J. Sound Vib.*, **230**(1), 171-125. <https://doi.org/10.1006/jsvi.1999.2608>.
- Lamb, H. (1921), “Axisymmetric vibration of circular plates in contact with water”, *Proc. R Soc. (London) A*, **98**, 205-216.
- Mandal, K.K. and Maity, D. (2015), “2d finite element analysis of rectangular water tank with separator wall using direct coupling”, *Coupl. Syst. Mech.*, **4**(4), 317-336. <https://doi.org/10.12989/csm.2013.2.2.127>.
- McLachlan, N.W. (1932), “The accession to inertia of flexible discs vibrating in a fluid”, *Proc. Phys. Soc. London*, **44**, 546-555.
- Schiffer, A. and Tagarielli, V.L. (2015), “The response of circular composite plates to underwater blast: Experiments and modelling”, *J. Fluid. Struct.*, **52**, 130-144. <https://doi.org/10.1016/j.jfluidstructs.2014.10.009>.
- Sorokin, S.V. and Chubinskij, A.V. (2008), “On the role of fluid viscosity in wave propagation in elastic plates

- under heavy fluid loading”, *J. Sound Vib.*, **311**, 1020-1038. <https://doi.org/10.1016/j.jsv.2007.10.001>.
- Wang, C., Fu, S. and Cui, W. (2009), “Hydroelasticity based fatigue assessment of the connector for a ribbon bridge subjected to a moving load”, *Marine Struct.*, **22**, 246-260. <https://doi.org/10.1016/j.marstruc.2008.06.009>.
- Wu, J.S. and Shih, P.Y. (1998), “Moving-load-induced vibrations of a moored floating bridge”, *Comput. Struct.*, **66**(4), 435-461. [https://doi.org/10.1016/S0045-7949\(97\)00072-2](https://doi.org/10.1016/S0045-7949(97)00072-2).

CC